Phys. Status Solidi A **207**, No. 4, 807–811 (2010) / **DOI** 10.1002/pssa.200983312

physica status solidi a
www.pss-a.com
applications and materials science

Surface chemistry and topographical changes of an electropolished NiTi shape memory alloy

Lakshman Neelakantan[1], Markus Valtiner[1], Gunther Eggeler[2], and Achim Walter Hassel*[,1,3]

[1] Max-Planck Institut für Eisenforschung, Max-Planck Str. 1, 40237 Düsseldorf, Germany
[2] Institut für Werkstoffe, Ruhr-Universität Bochum, Universitätsstraße 150, 44801, Bochum, Germany
[3] Institute for Chemical Technology of Inorganic Materials, Johannes Kepler University, Altenbergerstr. 69, 4040 Linz, Austria

Received 21 August 2009, revised 11 December 2009, accepted 22 December 2009
Published online 19 March 2010

Keywords polishing, etching, anodic films, electrodeposition, roughness, phase transformation

* Corresponding author: e-mail hassel@elchem.de, Phone: +43 732 2468 8704, Fax: +43 732 2468 8905

Electropolishing and its mechanism for NiTi shape memory alloy in methanolic sulfuric acid have been investigated recently. In the current study, X-ray photoelectron spectroscopy was carried out to characterize the chemical nature of the electropolished surface. The electropolished surface is covered by a thin layer of TiO_2. For an electropolished specimen, the Ni:Ti ratio at surface (~1 nm) was 0.31, whereas for a mechanically polished specimen the ratio was 0.70. The second aspect of this work is the attempt to characterize the salt film formed during electropolishing. The characterization of salt-film showed sulfide and sulfate compounds of Ni and/or Ti. The crystallographic and topographical changes caused due to thermally induced phase transformation on an electropolished NiTi was followed by *in situ* XRD and AFM. AFM studies revealed significant changes in the surface features due to phase transformation. The surface roughness value increased by a factor of 2.

1 Introduction Shape memory alloys such as NiTi show special mechanical properties like super-elasticity and shape memory effect [1]. They are widely used as biomaterials owing to their unique properties [2], however the biocompatibility of NiTi strongly depends on the surface stability. Numerous studies are available, which aim at improving the surface stability by different surface modification methods [3, 4]. Electropolishing of shape memory alloys is desirable from both biomedical and mechanical engineering point of view. Studies exist which describe electropolishing of NiTi as a modification method. Also, the performances of electropolished alloys were studied by various techniques [5–8]. However, a full pledged study on electropolishing behavior of NiTi and its mechanism was performed only in the recent past [9–11]. Fushimi et al. established the experimental conditions for electropolishing NiTi. Accordingly, electro-dissolution in a methanolic-3 M sulfuric acid solution, at a potential of 8 V and at a temperature of 263 K renders a bright, shiny and flat surface [11]. The underlying mechanism of electropolishing was investigated in a rotating disk electrode study [12]. This study revealed that the electro-dissolution is a mass transport limited process and hinted that dissolution products as the rate limiting species. Among the series of investigations related to electropolishing, an electrochemical impedance study performed under electropolishing condition revealed that electro-dissolution follows the salt film mechanism [13].

In the past, many authors have tried to ascertain the composition and properties of the salt film [14]. There is strong evidence that a salt film is present on the anode at the limiting current. Its thickness and physical properties are not well known but they apparently depend on the potential. Since the film disappears upon current switch off, it cannot be directly observed with *ex situ* methods. As reported in literature, it is difficult to isolate and analyze the anodic film formed under limiting current conditions, but still there are certain reports about attempts that have been made. Novak et al. [15] used ellipsometry to investigate anodic films formed during electropolishing of copper in phosphoric acid. A report by Fang et al. describes that the composition of the viscous liquid film in the electropolishing of Cu can be studied using XPS and AES [16].

Also, it is noteworthy to remember that NiTi being a shape memory alloy would undergo thermal or stress induced phase transformation. An electropolished surface is normally characterized in terms of a certain surface

morphology and roughness. Therefore, it is clear that phase transformations can cause considerable changes in surface morphology of an electropolished surface [9]. Moreover, the most obvious geometrical characteristics of a martensitic transformation are change in shape, shape deformation, or surface relief of a definite value. Sometimes this effect, *i.e.* the variation in surface roughness of an implant (*e.g.* NiTi orthodontic arch wires) due to phase transformation is overlooked by manufacturers [17].

Although electropolishing of NiTi in methanolic sulfuric acid and its mechanism is well established, still it is very important to explore the chemical change of the surface. Here, we report on the X-ray photoelectron spectroscopic (XPS) studies carried out on an electropolished surface. The second aspect of this work is the attempt made to identify the salt film composition. Finally, XRD and AFM measurements integrated with a heating stage allowed following the topographical changes due to phase transformation.

2 Experimental

2.1 Materials and electropolishing A NiTi alloy of composition 50.62 at.% Ni– 49.38 at.% Ti was used as specimen to follow the surface chemistry after electropolishing. The austenitic start temperature was (A_s) 293.5 K. To study the influence of phase transformation on the surface morphology of an electropolished surface, two different compositions of NiTi alloys were procured. These alloys exist either solely as a martensitic ($A_s = 343$ K) or as an austenitic phase ($A_s = 253$ K) at the temperature of electropolishing (263 K). Among the two, an alloy which exists in martensitic phase was chosen for the current study.

The specimens were mechanically ground using silicon carbide papers of various grades (up to 4 000), finally they were polished using diamond paste (3 μm followed by 1 μm) to a mirror finish. After polishing, the specimens were rinsed with distilled water, cleaned ultrasonically in ethanol, and dried. The test solution was a 3 M H_2SO_4 containing methanol which was prepared from analytical grade 95–97% sulfuric acid and methanol (pro analysis, Merck). Electropolishing was performed by holding the specimen at a potential of 8 V, at 263 K for 500 s [11]. To investigate the chemical nature of the salt film formed during electropolishing the specimen was withdrawn slowly without switching off the current and the surface of the specimen was immediately dried by air blast without any further cleaning treatment.

2.2 Characterization techniques Surface characterization was carried out using a Physical Electronics Quantum 2000 Scanning ESCA Microprobe. In order to ascertain the compositional variation and the oxide thickness, XPS sputter depth profiles were measured. The sputtering was performed with Ar^+ ions of energy 2 keV at a defined sputter rate. The sputter rate was calibrated by using an oxidized silicon wafer with known oxide thickness. In order to quantify the elemental depth profiles, CASA-XPS software with appropriate sensitivity factors was used. The elemental spectra were fitted with Gaussian–Lorentzian lines and Shirley background type. The field emission scanning electron microscope (FE-SEM, LEO 1550VP, GEMINI) equipped with an energy dispersive spectrometer for X-ray microanalysis (EDX) was used to investigate the morphology and the chemical composition of the deposited salt film.

The phase changes were determined by Grazing-incidence X-ray diffraction using a Bruker AXS D8 Advance equipped with a Göbel mirror and SolX detector. CuKα was used as X-ray source and the measurements were carried out with an incidence angle of 1°. A simple Peltier element was integrated as a heating stage. Prior to the start of the experiment, the Peltier element was calibrated for temperature as a function of the applied current. XRD spectra of the specimens were recorded for 2⊖ range of 20–70°, at a scan speed 0.08°/min with time per step of 10 s. The experiments were performed under ambient atmosphere. The (hkl) planes corresponding to the lines in XRD spectra were identified using the ICDD database incorporated in the Diffracplus EVA package provided by Bruker. Temperature controlled AFM measurements were performed using a JPK Nano Wizards AFM (JPK Instruments AG, Berlin, Germany). Contact mode was used to record the topographical changes caused due to the phase transformation.

3 Results and discussion

3.1 Surface chemistry after electropolishing

3.1.1 XPS characterization Figure 1 compares the XPS core level spectra of Ti2p, Ni2p, and S2p, obtained on the surface for a mechanically polished and an electropolished specimen. Figure 1a, a Ti2p spectrum shows that the surface is covered mainly with TiO_2 in both cases. Comparing the Ti2p signals it is seen that the concentration of Ti is higher at the electropolished surface. The oxide thickness for a mechanically polished surface was approximately 2.5 nm and that of an electropolished surface was 3.5 nm. Similar oxide thicknesses were reported earlier for NiTi surfaces modified by electropolishing [5–8]. Upon sputtering, the Ti2p signal shows gradual transition from Ti^{4+} to metallic Ti. This might be due to the presence of sub-oxides. Also, changes of the apparent valency caused by sputtering cannot be ignored [18]. However, an angle resolved XPS (ARXPS) analysis confirmed the presence of sub-oxides of Ti along with TiO_2.

Upon following the Ni2p spectrum at the surface from Fig. 1b, the electropolished specimen shows slightly higher concentration than that of the mechanically polished one. Nevertheless, the Ni: Ti ratio is lower when compared with a mechanically polished specimen. Hence it is confirmed that an electropolished surface is enriched with Ti.

The reason for slightly higher Ni concentration for electropolished surface can be explained by following the S2p signal (Fig. 1c). The S2p core level spectra show the presence of sulfate and sulfide compounds (probably Ni

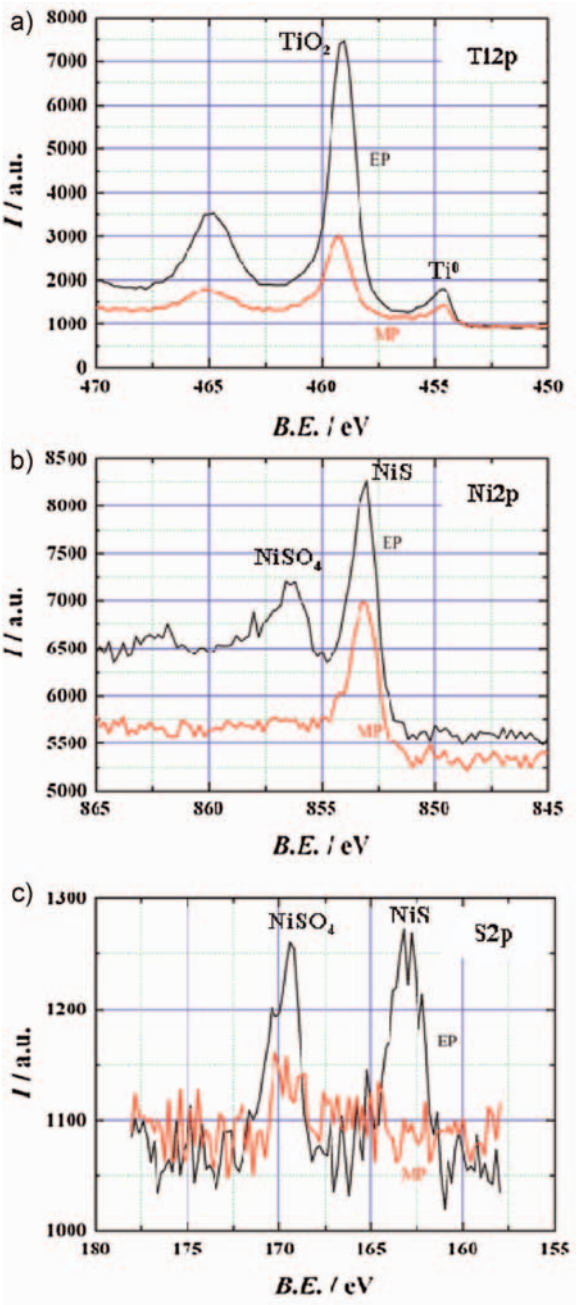

Figure 1 (online color at: www.pss-a.com) XPS core level spectra obtained on the surface of a mechanically polished and an electropolished NiTi. a) Ti2p, b) Ni2p and c) S2p. (EP = *electropolished* and MP = *mechanically polished* specimens).

compounds, as the Ni2p spectra indicates), which must have formed during electropolishing. The S2p spectrum from a mechanically polished surface shows no such peaks, hence the Ni peak in Fig. 1b is due to the presence of metallic Ni.

Strikingly, the presence of sulfate and sulfide compounds hints the possible chemical nature of the salt film that forms during electropolishing. It should be noted that electropolishing is performed in a methanolic sulfuric acid solution, hence the formation of sulfur compounds is

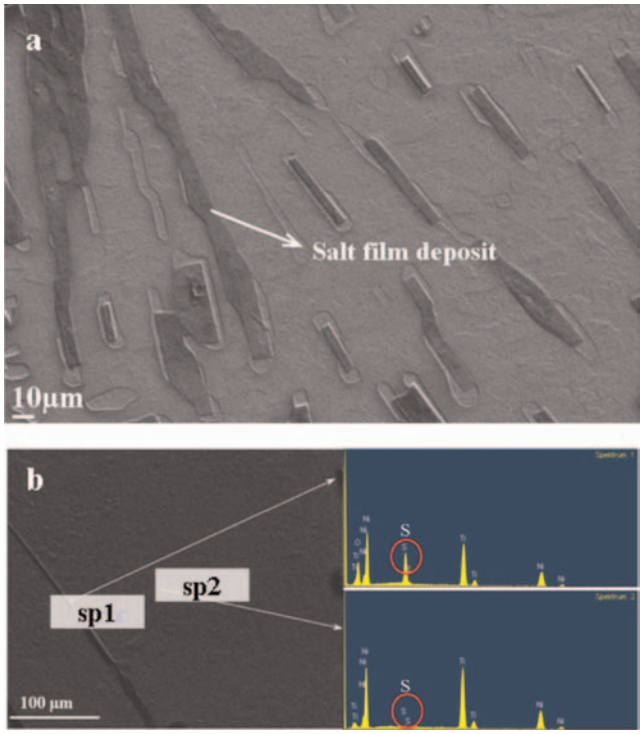

Figure 2 (online color at: www.pss-a.com) a) SEM micrograph showing deposits of salt film randomly deposited on the electropolished surface. b) EDX spectra obtained on the salt film deposit showing the dominance of the S signal.

obvious. Piotrowski et al. in their study on electropolishing of Ti assumed that the salt film formed could be a compound of titanium sulfate or methanolic titanium sulfate complex [19]. From the above XPS analysis, the assumption ascribed by Piotrowski et al. could also be valid for the NiTi system (Ni and/or Ti complex), however the exact stoichiometry is still tough to ascertain.

3.1.2 Compositional analysis of salt film The Ni2p spectrum represented in Fig. 1b hints that the salt film could be a sulfide/sulfate compound of Ni. Although sulfur compounds of Ti are not evident from the Ti2p peaks, still these compounds would have formed during electropolishing. These formed compounds might have been modified during air transfer. Figure 2a shows the morphology of the salt film deposited upon withdrawal of the specimen during current flow in the electropolishing process. The deposit is not homogenous throughout the surface, as it depends on the withdrawal itself. Figure 2b shows the EDX spectra collected at two different spots, one on the deposit and the other on the surface free of deposits. From the spectra 1 (sp1) it can be easily seen that the S signal is prominent as compared to the spectra 2. Heinrich and Feller investigated the electrical response of anodic films on nickel during electropolishing in methanolic H_2SO_4 by applying small potential steps and measuring the resulting current transients. The exact chemical composition of the films was not known but sulfate

and nickel ions were believed to be the main constituents in the film [20].

3.2 Surface changes due to transformation The room temperature stable phases namely the martensite and the austenite for the two different specimens were characterized using X-ray diffraction (XRD). Figure 3a shows the typical diffractogram corresponding to the martensitic and the austenitic phase respectively.

The X-ray diffractogram for austenite shows a high intense peak at 2θ 42.4° corresponding to the (110) plane. The crystal structure refers to a cubic structure and specifically to the CsCl structure (PDF: 03-065-7711). The X-ray diffractogram for the martensite phase shows characteristic multiple peaks at 2θ values of, 41.44, 44.08, 44.56, and 39.28°. Only four intense peaks are listed corresponding to a family of planes (-111), (020), (111), and (020) respectively. The pattern shows a monoclinic crystal structure typical for the martensitic phase (PDF No: 00-035-1281).

Figure 3b shows the follow up of the change in crystal structure of the specimen due to a thermally induced phase transformation. The parent phase at room temperature (30 °C) corresponds to martensite as shown by multiple reflections (as recorded in the earlier Fig. 3a). Upon increasing the temperature, the intensity of the martensite peaks decreases showing the process of transformation and at approximately 60 °C the peak corresponding to austenite arises. On further raising the temperature, the austenite peak becomes dominant with apparently no martensite peak remaining. XRD performed for the specimen at 87 °C shows a single high intense peak at 42.4°, which corresponds to the austenitic phase (the dominant phase).

The differential scanning calorimetric (DSC) results showed that the martensite to austenite phase transition temperature (A_s) was around 70 °C. This is also evident from the XRD studies.

Additionally this study by XRD is more sensitive compared to the thermal method like DSC as fractions of the phase change can be followed more precisely, suggesting the initial phase transformation starting at 60 °C. A similar kind of study on NiTi phase transformation using XRD was performed by Uchil et al. [21]. They formulated the technique to compare the DSC curves using the variation in peak intensity during phase transformation (upon cooling as well as heating).

The Fig. 4a shows the topography recorded by AFM at approximately 30 °C, where the surface is in the martensitic state. When heated to 80 °C (Fig. 4b), the alloy undergoes complete phase transformation. This can also be confirmed from Fig. 3b, where at 70 °C the reflections typical for austenitic phase can be seen. The phase transformation induces considerable changes in morphology and in roughness, which can be seen from the line profiles. The typical root mean square (rms) value of roughness for a specimen electropolished at the martensitic state is ∼ 16 nm, whereas upon phase transformation the rms value of roughness is ∼ 32 nm.

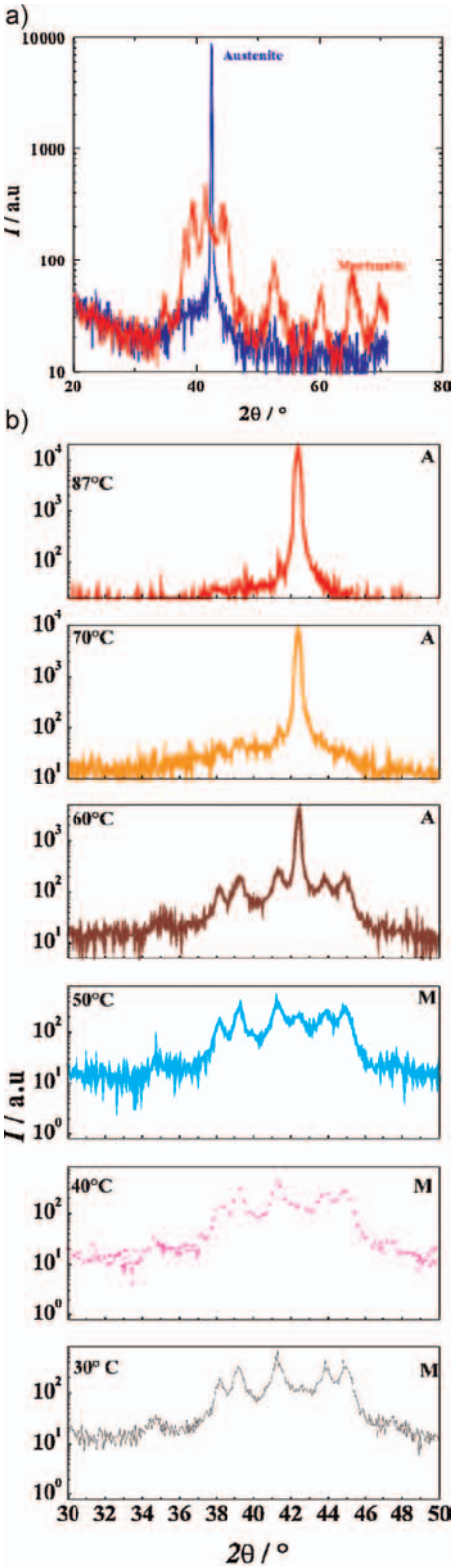

Figure 3 (online color at: www.pss-a.com) a) XRD pattern for typical martensite and austenite phase of two different NiTi specimens recorded at room temperature. b) XRD pattern, tracking the thermally induced phase transformation from martensite to austenite.

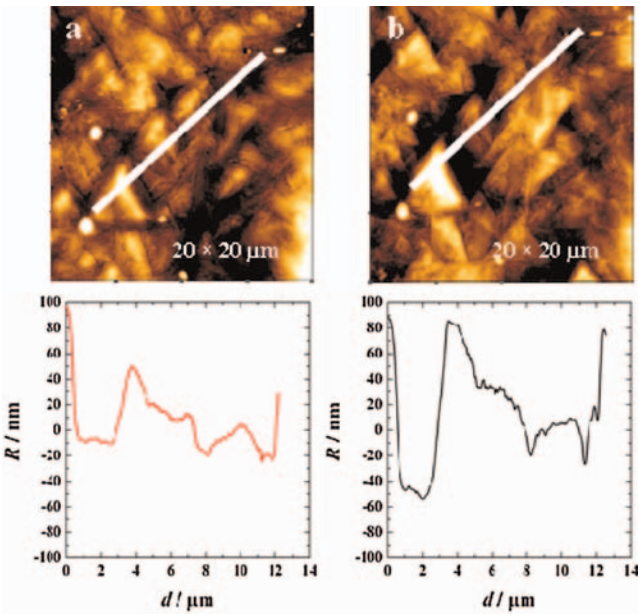

Figure 4 (online color at: www.pss-a.com) Topography and roughness changes caused by thermally induced phase transformation. Experiment was performed in an AFM integrated with a heating stage. a) Surface at 30 °C and b) surface at 80 °C.

Hence it is straightforward to deduce that phase transformation does lead to a change in surface roughness of an electropolished NiTi alloy. Normally in the absence of external load, the phase transformation results in no macroscopic shape change, but with an apparent surface relief. Heating the specimen well above the phase transformation temperature causes a complete transformation from martensite to austenite. On transformation to austenite phase, the specimen shows the presence of a pseudo-martensitic relief due to shearing, leading to considerable changes in the surface morphology and roughness [9]. As such, a flat surface (austenite) becomes rough upon cooling (twinned martensite) and *vice versa*. He et al. utilized a temperature controlled AFM to follow the phase transformation occurring on shape memory thin films [22].

Based on the fact that the surface roughness in a thermal cycle is associated with the ongoing phase transformation; it can also be used to determine the phase transformation temperature quantitatively from the surface roughness *versus* temperature relationship [22]. Pohl et al. in their work elucidated that a specimen structured this way would be beneficial for further processing like coating [9].

4 Conclusions The XPS depth profile reveals higher Ti concentration at the surface and near surface regions for an electropolished specimen compared to a mechanically polished one. The oxide layer is 2.5 and 3.5 nm for a mechanically and electropolished specimen, respectively. The binding state analysis for an electropolished specimen reveals Ti existing as TiO_2 on the surface. The depth profile shows the presence of sub-oxides of titanium. At the surface Ni exists in the form of sulfide and sulfate compounds. They are identified as the compounds of salt film most probably in the form of Ni and Ti sulfides and sulfates. The surface features namely morphology and roughness vary upon transformation. *In situ* temperature controlled XRD and AFM allows following surface changes caused due to phase transformation. The XRD characterization integrated with heating stage would allow following the phase transformation accurately. The AFM topographical study allows recording the changes accompanied with phase transformation.

Acknowledgements L.N acknowledges the International Max-Planck Research School-SurMat for the financial support. The authors wish to thank the Sonderforschungsbereich 459 of the Deutsche Forschungs Gemeinschaft for providing specimens of NiTi alloy. We acknowledge Dr. Srinivasan Swaminathan for his helpful discussions with XPS analysis.

References

[1] G. B. Kauffman and I. Mayo, J. Chem. Educ. **23**, 4863 (1996).
[2] T. Duerig, A. Pelton, and D. Stöckel, Mater. Sci. Eng. A **273–275**, 149 (1999).
[3] S. A. Shabalovskaya, Int. Mater. Rev. **46**, 1 (2001).
[4] A. W. Hassel, Min. Invas. Ther. Allied. Technol. **13**, 240 (2004).
[5] D. A. Armitage and D. M. Grant, Mater. Sci. Eng. A **349**, 89 (2003).
[6] B. Thierry, M. Tabrizian, C. Trepanier, O. Savadg, and L'H. Yahia, J. Biomed. Mater. Res. **49**, 88 (2000).
[7] S. Trigwell, R. D. Hayden, K. F. Nelson, and G. Selvaduray, Surf. Interface Anal. **26**, 483 (1998).
[8] C. Trepanier, M. Tabrizian, L'H. Yahia, L. Bilodeau, and D. L. Piron, J. Biomed. Mater. Res. **43**, 433 (1998).
[9] M. Pohl, C. Hessing, and J. Frenzel, Mater. Corros. **53**, 673 (2002).
[10] S. Barison, S. Cattarin, S. Daolio, M. Musiani, and A. Tuissi, Electrochim. Acta **50**, 11 (2004).
[11] K. Fushimi, M. Stratmann, and A. W. Hassel, Electrochim. Acta **52**, 1290 (2006).
[12] L. Neelakantan and A. W. Hassel, Electrochim. Acta **53**, 915 (2007).
[13] K. Fushimi, L. Neelakantan, G. Eggeler, M. Stratmann, and A. W. Hassel, in preparation.
[14] D. Landolt, Electrochim. Acta **32**, 1 (1987).
[15] M. Novak, A. K. N. Reddy, and H. Wroblowa, J. Electrochem. Soc. **117**, 733 (1970).
[16] J. L. Fang and N. J. Wu, J. Appl. Electrochem. **20**, 231 (1990).
[17] C. Bourauel, T. Fries, D. Drescher, and R. Plietsch, Eur. J. Orthod. **20**, 79 (1998).
[18] S. Hashimoto, A. Tanaka, A. Murata, and T. Sakurada, Surf. Sci. **556**, 22 (2004).
[19] O. Piotrowski, C. Madore, and D. Landolt, J. Electrochem. Soc. **145**, 2362 (1998).
[20] H. Heinrich and H. G. Feller, Metalloberfläche **38**, 267 (1984).
[21] J. Uchil, F. M. Braz Fernandez, and K. K. Mahesh, Mater. Charact. **58**, 243 (2007).
[22] Q. He, W. M. Huang, M. H. Hong, M. J. Wu, Y. Q. Fu, T. C. Chong, F. Chellet, and H. J. Du, Smart Mater. Struct. **13**, 977 (2004).